This article has been accepted for publication in IEEE Open Access Journal of Power and Energy. This is the author's version which has not been fully edited and content may change prior to final publication. Citation information: DOI 10.1109/OAJPE.2025.3549113

The Optimal Operation Strategy of an Energy Community Aggregator for Heterogeneous Distributed Flexible Resources

Xinyi Yang, Tao Chen, *Member, IEEE,* Yuanshi Zhang, *Member, IEEE,* Ciwei Gao, *Senior Member, IEEE,* Xingyu Yan, *Member, IEEE,* Hongxun Hui, *Member, IEEE,* Xiaomeng Ai, *Member, IEEE*

***Abstract*—The widespread integration of renewable energy into the grid emphasizes the issues of power system uncertainty and insufficient flexibility. Heterogeneous flexible distributed resources can address the above challenges by interacting with distribution networks. This paper proposes a multi-timescale optimal operation strategy for an energy community that aggregates multiple distributed resources. Based on flexibility indicators including the degree of load variation and task laxity, a tri-level structure involving distribution system operators (DSOs), aggregators, and the home energy management system (HEMS) is developed. The aggregator serves as mediator between customers and DSOs, gathering the end user's flexibility through the rescheduling of household appliances to leverage both upward and downward energy adjustments. According to different scenarios and application requirements, a multi-time-scale rolling optimal dispatch model is proposed. The day-ahead dispatch is combined with the Model Predictive Control (MPC) method to achieve fine-grained rolling adjustment of the power dispatch instructions of distributed resources with different time scales. Finally, a simulation experiment example is constructed to verify the effectiveness of the proposed method. The simulation results demonstrate that the economic benefits of end users and aggregators are improved with more grid-friendly load curves.**

***Index Terms*—Energy community, resource aggregator, flexible distributed resources, multi-level optimization, model predictive control.**

NOMENCLATURE

Indices and Sets

h_j	Index of houses h at bus j
j, k	Index of buses in distribution system, $(j,k) \in N$
t	Index of time, $t \in T$
$t_{h_j}^{\text{EV}}$	Index of time electric vehicle (EV) connected to house, $t_{h_j}^{\text{EV}} \in T$
$t_{h_j}^{\text{AR}}$	Index of time EV arrived to house, $t_{h_j}^{\text{AR}} \in T$
$t_{h_j}^{\text{DEP}}$	Index of time EV depart from house, $t_{h_j}^{\text{DEP}} \in T$

X. Yang, T. Chen, Y. Zhang, C. Gao and X. Yan are with the School of Electrical Engineering, Southeast University, Nanjing, China. (*Corresponding author*: Tao Chen, email: taoc@seu.edu.cn).

H. Hui is with the State Key Laboratory of Internet of Things for Smart City and Department of Electrical and Computer Engineering, University of Macau, Macao, China.

X. Ai is with the School of Electrical and Electronic Engineering, Huazhong University of Science and Technology, Wuhan, China.

This work is supported by National Natural Science Foundation of China under Grant No.52107079 and 52177088, Young Elite Scientists Sponsorship Program by Jiangsu Association for Science and Technology (JSTJ-2023-XH050) and "Zhishan Youth Scholar" Program of Southeast University under Grant No.2242023R40048.

Parameters

α	Solar elevation angle, rad
$\dot{v}_{h_j,t}$	The volumetric water flow rate, m^3/s
$\gamma_{h_j,t}^{\text{flex}}$	Flexibility index of each user, kW
$\left(P_{h_j,t}^{con}\right)_{J_1}$	Power demand using J_{1,h_j} , kW
$\left(P_{h_j,t}^{con}\right)_{J_2}$	Power demand using J_{2,h_j} , kW
$\pi_t^{\text{Buy}}, \pi_t^{\text{Sell}}$	Buying, selling price, $yuan/kWh$
ρ	The surface reflection coefficient of Building integrated photovoltaic (BIPV) array
$\theta_{j,k}$	Angle of complex Y-Bus matrix, rad
φ_m	The azimuth of BIPV array, rad
φ_s	Solar azimuth angle, rad
A	Extraterrestrial solar radiation intensity, W/m^2
C	The scattering coefficient of sky
C_u, C_m, C_l	The thermal capacitance of stratified Electric Water Heater (EWH)
k	The optical thickness factor
k_0	The temperature coefficient
K_{um}, K_{ml}	The modeled lumped thermal conductivity between every two nodes of EWH
m	The atmospheric mass
P^{pump}	Rated power of water pump at Water Treatment Station (WTS), kW
P_{stc}	Rated power of BIPV, kW
$P_{g_j}^{\min}, P_{g_j}^{\max}$	Lower, upper limit of active power generation, p.u
$P_{h_j,t}^{\text{BL}}$	Power of base load, kW
$P_{h_j,t}^{\max}$	The maximum power demand of user, kW
$P_{h_j,t}^{\text{flex}}$	The flexibility of each user, kW
$P_{j,t}^{\text{d}_{\text{agg}}}, P_{j,t}^{\text{sell}_{\text{agg}}}$	Aggregated power buy, sell from, to DSO, p.u
$P_{j,t}^{flex_{agg}}$	Total flexibility at bus j, kW
Q	Water volume injected per unit of operating power at WTS, m^3/kWh
$Q_{g_j}^{\min}, Q_{g_j}^{\max}$	Lower, upper limit of reactive power generation, p.u
$Q_{j,t}^{d_{agg}}$	Aggregated reactive power demand, p.u
$SoC_{t,i}^{\max}$	Maximum water volume level of WTS, m^3
$SoC_{t,i}^{\min}$	Minimum water volume level of WTS, m^3
$T_{\text{stc}}, G_{\text{stc}}$	The temperature and irradiance of BIPV cells in standard test conditions, °C, W/m^2
U_u, U_m, U_l	The thermal conductance of the tank insulation for stratified EWH

$V_j^{\min}, V_j^{\max}$ Minimum, maximum voltage at bus j, p.u
$Y_{j,k}$ Admittance of line of the electrical network, p.u
$\eta_{C_{h_j,t}}^{\text{EV}}, \eta_{D_{h_j,t}}^{\text{EV}}$ Charging, discharging efficiency of EV
$\eta_{i,k}$ The losses/leakages for each in-flow/outflow of reservoir, m^3
$E_{h_j,t}^{\text{EV, min}}, E_{h_j,t}^{\text{EV, max}}$ Minimum/Maximum energy level of Electric Vehicle (EV), kWh
$E_{h_j,t}^{\text{EV,AR}}, E_{h_j,t}^{\text{EV,DEP}}$ Arrival and departure energy of EV, kWh
$G_{j,k}$ Conductance between buses, p.u
$P_{Ch_j,t}^{\text{EV,max}}$ Maximum charging power of EV, kW
$P_{Dh_j,t}^{\text{EV,max}}$ Maximum discharging power of EV, kW
$p_{h_j,t}^{u,max}, p_{h_j,t}^{m,max}$ The Maximum power consumption of the EWH's heating element, W
$T_{\text{initial}}^u, T_{\text{initial}}^m, T_{\text{initial}}^l$ The initial water temperatures of stratified EWH, °C
$T_{h_j,t}^{\alpha}$ Ambient temperature, °C

Variables

$G_{h_j,t}$ Total solar radiation of BIPV, W/m^2
$P_{h_j,t}^{\text{BIPV}}$ Total power of BIPV, kW
$P_{t,i}^{\text{pump}}$ Power of water pump at WTS, kW
$X_{t,i}^{\text{WTS}}$ Status of the pump at WTS, ON/OFF
$E_{h_j,t}^{\text{EV}}$ Energy level of EV, kWh
$P_{C_{h_j,t}}^{\text{ESS}}$ Charging power of Energy Storage System (ESS), kW
$P_{C_{h_j,t}}^{\text{EV}}$ Charging power of EV, kW
$P_{D_{h_j,t}}^{\text{BIPV, DSO}}$ Power of PV supply to DSO, kW
$P_{D_{h_j,t}}^{\text{BIPV, ESS}}$ Power of PV supply to ESS, kW
$P_{D_{h_j,t}}^{\text{BIPV, H}}$ Power of PV supply to home, kW
$P_{D_{h_j,t}}^{\text{ESS,DSO}}$ Discharging power of ESS to DSO, kW
$P_{D_{h_j,t}}^{\text{ESS,H}}$ Discharging power of ESS to home, kW
$P_{D_{h_j,t}}^{\text{EV,DSO}}$ Discharging power of EV to DSO, kW
$P_{D_{h_j,t}}^{\text{EV,H}}$ Discharging power of EV to home, kW
$P_{D_{h_j,t}}^{\text{EV}}$ Total discharging power of EV, kW
$Q_{t,i,k}$ Water injected or discharged by other branches of WTS at step t, m^3
$SoC_{t,i}^{\text{WTS}}$ Water volume level of WTS at step t, m^3
$X_{h_j,t}^{\text{EV}}$ Charging and discharging status of EV, ON/OFF
$\delta_{k,t}, \delta_{j,t}$ Voltage angle at bus j, k, rad
$\pi_{h_j,t}^{\text{Inc}}$ Incentive and penalty, $yuan/kWh$
$P_{h_j,t}^{\text{Buy,DSO}}$ Buying power of household from DSO, kW
$P_{h_j,t}^{\text{Sell,DSO}}$ Selling power of household to DSO, kW
$P_{h_j,t}^{\text{EWH}}$ Power demand of stratified EWH, kW
$P_{h_j,t}^u, p_{h_j,t}^m$ The power consumption of the two heating elements, W
$X_{h_j,t}$ Status of buying and selling power, ON/OFF
$\phi_{h_j,t}^{EV}$ The laxity of EV
$P_{j,t}^{f_{\text{DSO}}}, Q_{j,t}^{f_{\text{DSO}}}$ Active, reactive flexibility signal, p.u
$P_{j,t}^g, Q_{j,t}^g$ Active, reactive power generation, p.u
$T_{h_j,t}^u, T_{h_j,t}^m, T_{h_j,t}^l$ The water temperatures of stratified EWH, °C
$V_{j,t}, V_{k,t}$ The voltage level at bus j and k, p.u

I. Introduction

With the rapid development and construction of power systems, the high penetration of renewable energy sources causes an increase in the volatility of power generation and the uncertainty of the grid. At the same time, the supply-demand imbalance in the system should be taken seriously and it is difficult to achieve the balance of power supply and demand only by power supply regulation [1]. In smart grid, Advanced Metering Infrastructures (AMI) do not only allow monitoring the energy consumption or generation for billing purposes, but also provide useful power quality information [2]. Through two-way communication facilities and AMI [3], the bi-directional flow of electric power between traditional generation units on the supply side and distributed energy resources(DERs) on the demand side has been possible [4] [5]. As a result, exploring the potential flexibility on the user side, integrating dispersed demand-side flexible distributed resources and achieving centralized dispatch with flexibility have become a new solution for energy management strategies in new power systems [6] [7].

When a customer connected to the distribution grid which has any combination of consuming, producing, or energy storing devices at its premises, the customer has production capabilities and becomes prosumer. Prosumers have the ability to adjust their resource allocation by either reducing electricity demand or shifting their loads to other periods of the day [8] [9]. The participation of prosumers has been studied in the field of smart grids with the aim of managing DERs owned by prosumers to reduce their electricity bills while improving system operational flexibility [10]. In addition to traditional distributed resources, amounts of new flexible resource such as building integrated photovoltaic (BIPV) [11] [12], water treatment station (WTS) [13], and electric water heater (EWH) [14] [15] with tank stratification, can jointly participate in the centralized dispatch [16]. The prosumers can provide flexibility to the grid by changing their power profiles by modifying household appliance behavior using a HEMS.

Numerous DERs are scattered on the demand side, so the intelligent aggregation and regulation of flexibility resources are hard to achieve. The aggregator becomes an essential participant in this scenario, which can gather overall flexibility from groups of prosumers and decrease the burden on the communication network significantly [17]. In [18], an optimization-based home energy management system was proposed to schedule the consumption of controllable home appliances. However, it did not examine how the management of DERs impacts the operation of the distribution grid. A two-stage optimization framework that includes residential energy hubs and local distribution operators, was proposed in [19], without considering the role of aggregators. Reference [20] proposed an aggregator model for managing home energy management system (HEMS) within an energy community and was only focused on transferable loads and uncontrolled loads. In [21], the researchers have defined a trilevel energy pricing model for demand-side management based on the time of use (ToU) price. The work proposed in [22] addressed the dilemma of coordination between three types of stakeholders,

This article has been accepted for publication in IEEE Open Access Journal of Power and Energy. This is the author's version which has not been fully edited and content may change prior to final publication. Citation information: DOI 10.1109/OAJPE.2025.3549113

namely smart distribution networks, microgrids, and customers with DERs under a comprehensive trilevel framework, and two coordination schemes were formulated to analyze interactions between the smart distribution network and microgrids with DERs. Consequently, it is imperative to investigate the coordination among DSOs, aggregators, and prosumers, which can lower energy costs for prosumers, and minimize network losses and peak power demand by utilizing the flexibility of prosumers. Strategies must be constructed to effectively utilize the flexibility of consumers within a reliable and efficient distribution system.

Quantifying the general characteristics of the flexibility resource clusters is a crucial prerequisite to assess the response capacity of DERs [23]. The concept of "flexibility" was explained and a method was proposed to classify the characteristics of flexibility resources in [24]. Flexibility can also be defined as the potential load variation of a user within a given time interval, which can be offered to the DSO for system balancing [19]. In [25], flexibility factor, namely laxity, is the difference between the amount of time remaining to complete the task and the time required to complete it at its maximum rate. A distributed coordinative transaction mechanism of a community integrated energy system was recommended in [26] with utilizing a tri-level game model. Based on the flexibility, the researchers [27] suggested a three-level framework with a novel incentive program to aggregate and coordinate the contributions of a large number of DERs, which can provide flexibility services to the DSO. However, a common limitation across these studies is the day-ahead scheduling of DERs, lacking real-time strategy. Also, most studies only focus on the evaluation of demand flexibility by using a single indicator and ignore the effect of other flexibility index across various application scenarios [28]. Therefore, the energy management of DERs should consider the uncertainty of the forecasted values used in the model and the symthetic effect of flexibility factors.

Model predictive control (MPC) has recently gained more popularity in the field of building and solving optimal control models for energy management. Reference [29] presented a model for real-time scheduling of combined heat production and electrical energy production for a residential microgrid based on MPC. In [30] [31], Each microgrid is equipped with an MPC-based energy management system, responsible for optimally controlling flexible loads, heating systems, and local generation devices based on operational constraints. Another study [32] proposed an appliance scheduling scheme for residential building energy management controllers, by exploiting operational flexibilities of thermal and non-thermal appliances using a MPC method. However, the authors primarily use MPC-based energy management system while ignoring the the impact of flexibility on the operation of energy community. Aiming at the coordinated control of the sources, a multi-time scale collaborative optimization strategy of multi-source based on MPC and flexibility indicators should be considered.

Based on the above discussion, it can be seen that much more work is needed in the combined effect of multiple factors and the energy coordination framework with the integration of three-stage energy management systems. There is also much more work required to study how to achieve the more precise control with a multiple time-scale dispatch model.

Thus, the contribution of this paper can be summarized as follows:1) introduce a detailed electric model of heterogeneous distributed flexible resources, extend and improve the mathematical model of the HEMS considering the interactions with aggregator and DSO; 2) propose an optimal operation strategy and an adaptive incentive program based multiple indicators including the flexibility of load variation and the task laxity, and perform unified energy management for resources with a more grid-friendly load curve and better economic benefits; 3)explore a multi-time scale dispatch model using MPC methods, which combines day-ahead scheduling with rolling optimization to achieve forward-looking and step-by-step regulation of the three-stage energy management system.

II. System Architecture and Mathematical Model

This section introduces the assumptions and mathematical modeling of the energy community, including DSO, aggregator and HEMS, as is illustrated in Fig. 1.

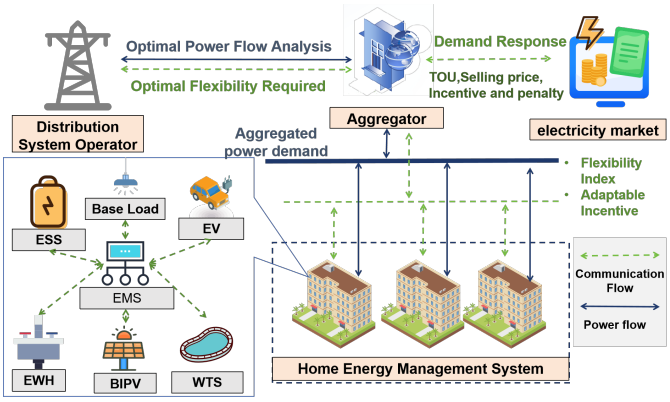

Fig. 1: Conceptual diagram of Energy Community

A. Home Energy Management System (first stage)

In this study, each household has an Electric Vehicle (EV), BIPV, Energy Storage System (ESS), WTS and EWH, controlled by a HEMS, accommodating each customer's preferences and objectives. Other appliances such as the refrigerator, lighting system do not provide full flexibility to the DSO and are referred to as base loads. The goal of the HEMS is assumed to be minimizing electricity consumption costs while fulfilling various demands for DERs scheduling and user preferences.

Objective Functions:

Three different objectives are used for the multiple HEMSs considered in this paper.

Minimize Cost: The objective of user h_j located at bus j is to minimize its total cost of energy, net of revenue earned. With the advent of dynamic pricing and smart meters, customers seek to minimize their cost or choose any other objective criterion. In this case, the load profile is referred to as the "desired load profile", which can be calculated by using J_{1,h_j}.

$$J_{1,h_j} = \sum_{t \in T} \left(P_{h_j,t}^{\text{Buy,DSO}} \cdot \pi_t^{\text{Buy}} - P_{h_j,t}^{\text{Sell,DSO}} \cdot \pi_t^{\text{Sell}} \right) \tau \qquad (1)$$

Where $P_{h_j,t}^{\text{Buy,DSO}}$ indicates the power imported from DSO at time t with the price π_t^{Buy}. $P_{h_j,t}^{\text{Sell,DSO}}$ is the power selling to the grid from the HEMS corresponding to the selling price π_t^{Sell}. τ represents time step, taken as 15min in this paper.

Minimize Energy Consumption and Maximize Task Laxity: The end-user minimizes its total energy consumption of the household appliances and maintains adequate task flexibility for all active tasks across the time horizon. Before the emergence of smart meters and dynamic pricing schemes, customers were billed at a flat rate for their electricity consumption; hence, customers sought to minimize their daily total energy consumption. This load profile is referred to as the "baseline" demand, which is the power demand of the user using J_{2,h_j}.

$$\begin{aligned} J_{2,h_j} = & \sum_{t\in T}\Big(P_{h_j,t}^{\text{BL}} + P_{h_j,t}^{\text{EWH}} + P_{h_j,t}^{\text{WTS}} + \Big(P_{C_{h_j,t}}^{\text{EV}} - P_{D_{h_j,t}}^{\text{EV,H}}\Big) \\ & + \Big(P_{C_{h_j,t}}^{\text{ESS}} - P_{D_{h_j,t}}^{\text{ESS, H}}\Big) - P_{D_{h_j,t}}^{\text{BIPV,H}}\Big)\tau \\ & + \sum_{t\in T}\Big(NT - \phi_{h_j,t}^{EV}\Big)^2 \end{aligned} \tag{2}$$

The right-hand side of equation (2) is the power demand of the base load, the power demand of EWH and WTS , charging of EV and ESS, and the power supply to the household from the EV, ESS, and PV, respectively. The last term in (2) maximizes task laxities at subsequent time steps within the horizon, which will be discussed in the following subsections.

Minimize Cost with incentive program: After receiving a flexibility request from the DSO, HEMS performs optimization based on the flexibility requirements utilizing new constraints and objective functions.

$$\begin{aligned} J_{3,h_j} = & \sum_{t\in T}\Big(P_{h_j,t}^{\text{Buy, DSO}} \cdot \pi_t^{\text{Buy}} - P_{h_j,t}^{\text{Sell,DSO}} \cdot \pi_t^{\text{Sell}} \\ & - \pi_{h_j,t}^{\text{Inc}} \cdot P_{h_j,t}^{\text{Buy,DSO}}\Big)\tau \end{aligned} \tag{3}$$

Where, $\pi_{h_j,t}^{\text{Inc}}$ is the flexible adaptive incentive program, which will be discussed in detail in Sections I-A-6).

HEMS Mathematical Model:

1) Building Integrated Photovoltaic: BIPV combines photovoltaic power generation units with buildings and has a series of advantages, such as reducing building construction costs and saving land resources on the ground. Hence, it's in line with the trend for green building development today [33].

$$P_{h_j,t}^{\text{BIPV}} = P_{\text{stc}}\frac{G_{h_j,t}}{G_{\text{stc}}}\left[1 + k_0\left(T_{h_j,t}^{\alpha} - T_{\text{stc}}\right)\right] \forall t \in T; \forall h_{j,t} \in H \tag{4}$$

In (4), the output power of BIPV is determined by the intensity of solar radiation and environmental temperature. The amount of solar radiation $G_{h_j,t}$ received by the surface of an object consists mainly of direct, scattered and reflected radiation, which is calculated as follows.

$$\begin{aligned} G_{h_j,t} = & Ae^{-km}\left(\cos\alpha\sin\beta\cos\left(\varphi_m - \varphi_s\right) + \sin\alpha\cos\beta\right) \\ & + Ae^{-km}\rho(\sin\beta + C)\left(\frac{1-\cos\beta}{2}\right) \\ & + ACe^{-km}\left(\frac{1+\cos\beta}{2}\right) \quad \forall t \in T; \forall h_{j,t} \in H \end{aligned} \tag{5}$$

Where β represents the tilt angle of the photovoltaic array operated in the range between 0 and $\pi/2$. BIPVs can achieve regulation of photovoltaic power generation by changing the tilt angle β in real time to more in line with the user's needs.

HEMS distributed the power generated by the BIPV to the DSO, ESS and the house is described in (6).

$$P_{h_j,t}^{\text{BIPV}} = P_{D_{h_j,t}}^{\text{BIPV, DSO}} + P_{D_{h_j,t}}^{\text{BIPV, ESS}} + P_{D_{h_j,t}}^{\text{BIPV,H}} \quad \forall t \in T; \forall h_j \in H \tag{6}$$

2) Water Treatment Station: WTS is an indispensable load resource for residential communities. The water pumps are the most energy intensive components, which are responsible for transferring water between water reservoirs. The flexibility potential lies in the ability to take advantage of the storage capacity of the reservoirs to schedule pump operation in the most cost-effective way.

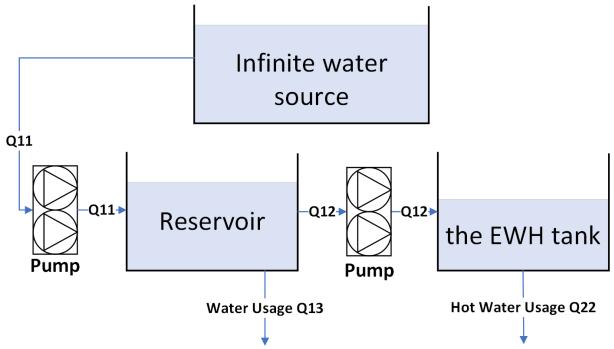

Fig. 2: Schematic of a generic water treatment station

There are two main building blocks in this WTS model, namely the reservoirs and the water flows that enter in or exit from the reservoirs as is illustrated in Fig. 2. The model is as follows [13]:

$$SoC_{t+1,i}^{\text{WTS}} = SoC_{t,i}^{\text{WTS}} + \sum_{k=1}^{K} Q_{t,i,k}\eta_{i,k} \quad \forall t \in T; \forall h_j \in H \tag{7}$$

$$Q_{t,i,k} = Q \cdot X_{t,i}^{WTS} \quad \forall t \in T; \forall h_j \in H \tag{8}$$

$$SoC_{t,i}^{\min} \le SoC_{t,i}^{\text{WTS}} \le SoC_{t,i}^{\max} \quad \forall t \in T; \forall h_j \in H \tag{9}$$

$$P_{t,i}^{\text{pump}} = P^{\text{pump}} \cdot X_{t,i}^{WTS} \quad \forall t \in T; \forall h_j \in H \tag{10}$$

$X_{t,i}^{WTS}$is a binary variable that involves the start-up or shutdown of the unit. Infinite water source, Reservoirs and the EWH tank are connected with water flows that can be controllable by a set of pumps. Equation (7) delineates the evolution of the state of charge (SOC). Constraint (9) sets the upper and lower limits of WTS's SOC, while (10) imposes restrictions on the maximum operating power of the water pump within WTS.

3) Electric Water Heater: Considering the size of the storage tanks of water heaters, most residential water heater tanks are designed with thermal stratification to improve energy efficiency. In this section we propose a three-node thermal model of EWH that coarsely accounts for tank stratification while remaining computationally tractable.

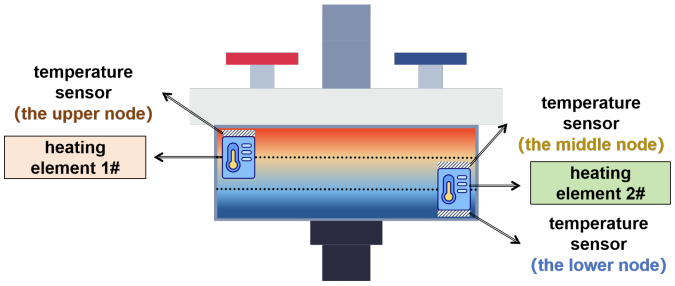

Fig. 3: Three-node water heater thermal model

The model assumes that there are three stratified volumes of water inside the EWH, each with a different temperature as is illustrated in Fig. 3. In general, two-element resistive water heaters with two temperature sensors has temperature profiles in three distinct, relatively well-mixed regions: (i) above the upper element, (ii) between the two elements, and (iii) below the lower element. Under buoyancy, these temperature regions tend to be well mixed, if the heating elements have been in operation for a period of time. The temperature will become less homogeneous after large water withdrawals or after long periods without power consumption. It is assumed that the upper and middle temperatures are measured using the sensors above each element, and the lower temperature is measured using the sensor below the lower element.

Considering these factors, the EWH model can be summarized as follows:

$$T^u_{h_j,t+1} = f_u\left(T^u_{h_j,t}, T^m_{h_j,t}, P^u_{h_j,t}\right) \quad \forall t \in T; \forall h_{j,t} \in H \tag{11}$$

$$T^m_{h_j,t+1} = f_m\left(T^u_{h_j,t}, T^m_{h_j,t}, T^l_{h_j,t}, P^m_{h_j,t}\right) \forall t \in T; \forall h_{j,t} \in H \tag{12}$$

$$T^l_{h_j,t+1} = f_l\left(T^m_{h_j,t}, T^l_{h_j,t}\right) \forall t \in T; \forall h_{j,t} \in H \tag{13}$$

$$T^l_{h_j,t} \le T^m_{h_j,t} \le T^u_{h_j,t} \quad \forall t \in T; \forall h_{j,t} \in H \tag{14}$$

$$0 \le p^m_{h_j,t} \le p^{m,max}_{h_j,t} \quad \forall t \in T; \forall h_{j,t} \in H \tag{15}$$

$$0 \le p^u_{h_j,t} \le p^{u,max}_{h_j,t} \quad \forall t \in T; \forall h_{j,t} \in H \tag{16}$$

$$T^u_{h_j,t} = T^u_{\text{initial}} \quad t = 0, \forall h_j \in H \tag{17}$$

$$T^m_{h_j,t} = T^m_{\text{initial}} \quad t = 0, \forall h_j \in H \tag{18}$$

$$T^l_{h_j,t} = T^l_{\text{initial}} \quad t = 0, \forall h_j \in H \tag{19}$$

$$P^{\text{EWH}}_{h_j,t} = (p^m_{h_j,t} + p^u_{h_j,t})/1000 \quad \forall t \in T; \forall h_{j,t} \in H \tag{20}$$

Equations (15) and (16) are constraints on the power of the heating element, limiting the maximum power. Equations (17) - (19) define the initial temperature, while (14) ensure that the temperature conditions hold. Equations (11) - (13) define the system dynamics in discrete time. In continuous time, the temperature dynamics of the three node are modeled as:

$$T^u_{h_j,t+1} = \left[\frac{U_u}{C_u}\left(T^\alpha_{h_j,t} - T^u_{h_j,t}\right) - \frac{\dot{v}_{h_j,t}}{V_u}\left(T^u_{h_j,t} - T^m_{h_j,t}\right) + \frac{P^u_{h_j,t}}{C_u} + \frac{K_{um}}{C_u}\left(T^m_{h_j,t} - T^u_{h_j,t}\right)\right]\tau + T^u_{h_j,t} \tag{21}$$

$$T^m_{h_j,t+1} = \left[\frac{U_m}{C_m}\left(T^\alpha_{h_j,t} - T^m_{h_j,t}\right) - \frac{\dot{v}_{h_j,t}}{V_m}\left(T^m_{h_j,t} - T^l_{h_j,t}\right) + \frac{P^m_{h_j,t}}{C_m} + \frac{K_{ml}}{C_m}\left(T^l_{h_j,t} - T^m_{h_j,t}\right) + \frac{K_{um}}{C_m}\left(T^u_{h_j,t} - T^m_{h_j,t}\right)\right]\tau + T^m_{h_j,t} \tag{22}$$

$$T^l_{h_j,t+1} = \left[\frac{U_l}{C_l}\left(T^\alpha_{h_j,t} - T^l_{h_j,t}\right) - \frac{\dot{v}_{h_j,t}}{V_l}\left(T^l_{h_j,t} - T_i\right) + \frac{K_{ml}}{C_l}\left(T^m_{h_j,t} - T^l_{h_j,t}\right)\right]\tau + T^l_{h_j,t} \tag{23}$$

In (21)-(23), the water temperature variation of EWH is seen as a function of ambient losses, uniform flow from the bottom to the top of the tank, conduction between adjacent nodes, and heating by the two elements.

4) Electric Vehicle and Energy Storage System: EVs are flexible energy-intensive loads with the ability to charge and discharge multiple times within a scheduling period. Since EV and ESS both contain the battery, they have similar operation constraints [34].In this paper, the following model is developed by considering the charging and discharging characteristics of EV:

$$E^{\text{EV}}_{h_j,t} = E^{\text{EV}}_{h_j,t-1} + \tau\left(P^{\text{EV}}_{C_{h_j,t}} \cdot \eta^{\text{EV}}_{C_{h_j,t}} - P^{\text{EV}}_{D_{h_j,t}}\right) \quad \forall t \in t^{\text{EV}}_{h_j}; \forall h_j \in H \tag{24}$$

$$P^{\text{EV}}_{D_{h_j,t}} = \frac{P^{\text{EV,DSO}}_{D_{h_j,t}} + P^{\text{EV,H}}_{D_{h_j,t}}}{\eta^{\text{EV}}_{D_{h_j,t}}}, \quad \forall t \in t^{\text{EV}}_{h_j}; \forall h_j \in H \tag{25}$$

$$0 \le P^{\text{EV}}_{Ch_j,t} \le P^{\text{EV,max}}_{Ch_j,t} \cdot X^{\text{EV}}_{h_j,t} \quad \forall t \in t^{\text{EV}}_{h_j}; \forall h_j \in H \tag{26}$$

$$0 \le P^{\text{EV}}_{Dh_j,t} \le P^{\text{EV,max}}_{Dh_j,t} \cdot \left(1 - X^{\text{EV}}_{h_j,t}\right) \quad \forall t \in t^{\text{EV}}_{h_j}; \forall h_j \in H \tag{27}$$

$$E^{\text{EV, min}}_{h_j,t} \le E^{\text{EV}}_{h_j,t} \le E^{\text{EV,max}}_{h_j,t} \quad \forall t \in t^{\text{EV}}_{h_j}; \forall h_j \in H \tag{28}$$

$$E^{EV}_{h_j,t} = E^{EV,AR}_{h_j,t} \quad \forall t \in t^{AR}_{h_j}; \forall h_j \in H \tag{29}$$

$$E^{EV}_{h_j,t} = E^{EV,DEP}_{h_j,t} \quad \forall t \in t^{DEP}_{h_j}; \forall h_j \in H \tag{30}$$

Equation (24) describes the power level of the EV, and (25) describes that when the EV is plugged in at home, it can discharge to the user's other appliances or sell electricity to the DSO. $X^{\text{EV}}_{h_j,t}$ is defined as a binary variable, with 1 indicating charging and 0 indicating either selling power to the grid or discharging to other appliances. Constraint (26) and (27) limit the charging and discharging power of the EV, ensuring that charging and discharging do not occur simultaneously. Constraint (29) and (30) define the energy levels at the time of arrival and departure.

5) General Power Management Strategy: Equation (31) ensures that the net power consumption of appliances is equal to the power purchased from DSO.

$$P_{h_j,t}^{\text{Buy,DSO}} = P_{h_j,t}^{BL} + P_{h_j,t}^{\text{EWH}} + \left(P_{C_{h_j,t}}^{\text{EV}} - P_{D_{h_j,t}}^{\text{EV,H}}\right) - P_{D_{h_j,t}}^{\text{BIPV,H}} + P_{h_j,t}^{\text{WTS}} + \left(P_{C_{h_j,t}}^{\text{ESS}} - P_{D_{h_j,t}}^{\text{ESS,H}}\right) \quad \forall t \in T; \forall h_j \in H \tag{31}$$

HEMS can also sell electricity power to DSO and make a profit according to the feed-in tariff (FiT).

$$P_{h_j,t}^{\text{Sell,DSO}} = P_{D_{h_j,t}}^{\text{EV, DSO}} + P_{D_{h_j,t}}^{\text{ESS, DSO}} + P_{D_{h_j,t}}^{\text{BIPV, DSO}} \quad \forall t \in T; \forall h_j \in H \tag{32}$$

Equation (33) and (34) ensure that the processes of selling and buying electricity do not occur simultaneously. M is a very large number. Mathematically, the functional state of HEMS can be easily modeled using a binary variable $X_{h_j,t}$ that is equal to 0 or 1 depending on whether the unit is buying or selling electricity respectively.

$$0 \leq P_{h_j,t}^{\text{Buy,DSO}} \leq M \cdot X_{h_j,t} \quad \forall t \in T; \forall h_{j,t} \in H \tag{33}$$

$$0 \leq P_{h_j,t}^{\text{Sell, DSO}} \leq M \cdot \left(1 - X_{h_j,t}\right) \forall t \in T; \forall h_{j,t} \in H \tag{34}$$

6) Flexibility Definition and Evaluation: :

a) Flexibility: Based on the above definitions and models, the flexibility available from a user, at a given time interval, is defined as the difference between the "desired load profile" and the "base line demand", given as follows:

$$P_{h_j,t}^{\text{flex}} = \left(P_{h_j,t}^{con}\right)_{J_1} - \left(P_{h_j,t}^{con}\right)_{J_2} \forall t \in T; \forall j \in N \tag{35}$$

Mathematically, the flexibility of each user is defined as the difference between power demand by each user using objective function J_{1,h_j} and J_{2,h_j}. If the power demand of the user using J_{1,h_j} is greater than power demand using J_{2,h_j}, then the user can provide upward flexibility to the grid, which means that the user can reduce power demand. Similarly, if the power demand using J_{1,h_j} is less than the power demand of J_{2,h_j}, users provide downward flexibility to the grid, indicating that the user needs more electricity from the grid.

Based on the flexibility of each user, this paper adopts an adaptable incentive scheme instead of a fixed incentive based on demand response. It can be calculated based on the flexibility provided by each user, and each user will have different rewards or penalties depending on their electricity demand. The formula for calculating novel incentives is as follows:

$$\pi_{h_j,t}^{\text{Inc}} = (\alpha - \beta)\left(\frac{\exp\left(\left(P_{h_j,t}^{con}\right)_{J_2} - \left(P_{h_j,t}^{con}\right)_{J_1}\right)}{\exp\left(\left(P_{h_j,t}^{con}\right)_{J_2} - \left(P_{h_j,t}^{con}\right)_{J_1}\right) + 1}\right) + \beta \quad \forall t \in T; \forall h_j \in H \tag{36}$$

where α is the maximum incentive (0.8 yuan/kWh) and β is the maximum penalty (0.6 yuan/kWh). If the desired power demand $\left(P_{h_j,t}^{con}\right)_{J_1}$ is less than the baseline demand demand $\left(P_{h_j,t}^{con}\right)_{J_2}$, the user will increase their power demand and receive an incentive. Similarly, if the desired power is greater than the baseline demand, the user will decrease power demand and be penalized to prevent the excessive growth of demand.

b) Laxity: Deferrable Loads require a certain energy delivered over a specified time interval, and its power demand can be modeled as tasks T_i. The energy management system can delay the execution of a task for a certain period of time after receiving it, so we use the maximum deferrable time to quantify the degree of flexibility in scheduling tasks.

Laxity is defined as the difference between the remaining time and the minimum time required to fulfil the task requirements. This is a measure of the degree of deferrability in scheduling a task, and tasks with greater laxity provide greater scheduling flexibility. The maximum deferrable time and the laxity for each task T_i are defined as:

$$\delta_i(t) = d_i - \frac{e_i(t)}{m_i} \tag{37}$$

$$\phi_i(t) = (d_i - t) - \frac{e_i(t)}{m_i} = \delta_i(t) - t \tag{38}$$

Deferrable loads such as EVs usually have charging and discharging deadlines, so in this paper we use laxity to optimize the charging and discharging times of EVs, which is calculated as follows:

$$\phi_{h_j,t}^{\text{EV}} = \left(t_{h_j}^{\text{DEP}} - t\right) - \frac{E_{h_j,t}^{\text{EV, DEP}}}{P_{Ch_j,t}^{\text{EV,max}}} = \delta_{h_j,t}^{\text{EV}} - t \quad \forall t \in t_{h_j}^{EV}; \forall h_j \in H \tag{39}$$

B. Aggregator Model (second stage)

As an intermediary between multiple users and DSO, the aggregator evaluates the demand response potential of users through professional technical evaluations and integrates dispersed demand response resources to participate in power system operations.

In this paper, we assume that aggregation is defined as the summation of power demands. The aggregator sums the buying and selling power of the houses as follows:

$$P_{j,t}^{d_{agg}} = \sum_{h}^{H} P_{h_j,t}^{\text{Buy, DSO}} \quad \forall t \in T; \forall j \in N \tag{40}$$

$$P_{j,t}^{\text{sell}_{\text{agg}}} = \sum_{h}^{H} P_{h_j,t}^{\text{Sell,DSO}} \quad \forall t \in T; \forall j \in N \tag{41}$$

The net flexibility of HEMS is calculated by taking the sum of downward and upward flexibility. The total flexibility of a bus is the sum of the flexibility for all customers connected at the bus, given by $P_{j,t}^{\text{flex}_{\text{agg}}}$ in (42). The user flexibility index $\gamma_{h_j,t}^{\text{flex}}$ in (43), is obtained by normalizing the flexibility of a customer by the total flexibility at that bus.

$$P_{j,t}^{\text{flex}_{\text{agg}}} = \sum_{h}^{H} P_{j,t}^{\text{flex}} \quad \forall t \in T; \forall j \in N \tag{42}$$

$$\gamma_{h_j,t}^{\text{flex}} = \frac{P_{h_j,t}^{\text{flex}}}{P_{j,t}^{\text{flex}_{\text{agg}}}} \quad \forall t \in T; \forall h_j \in H; \forall j \in N \tag{43}$$

The aggregator can calculate the maximum power limit according to the flexibility of each user as follows:

$$P_{h_j,t}^{\max} = \left(P_{h_j,t}^{con}\right)_{J_1} - \gamma_{h_j,t} P_{j,t}^{f_{\text{DSO}}} \quad \forall t \in T; \forall h_j \in H; \forall j \in N \tag{44}$$

The maximum power limit will be an additional constraint when re-run the HEMS optimization, as shown in (45).

$$P_{h_j,t}^{\text{Buy,DSO}} \leq P_{h_j,t}^{\max} \quad \forall t \in T; \forall h_j \in H \tag{45}$$

C. DSO Model (third stage)

The Distribution System Operator (DSO) primarily performs optimal power flow analysis for distribution systems with the goal of reducing overall transmission losses and fulfilling the requirements for optimal flexibility. The optimization objectives of DSO are as follows:

$$\begin{aligned} J_{4,h_j} = \sum_{t \in T} \Bigg(& \frac{1}{2} \sum_{j=1}^{N} \sum_{k=1}^{N} G_{j,k} \left(V_{j,t}^2 + V_{k,t}^2 \right. \\ & \left. -2V_{j,t}^2 \cdot V_{k,t}^2 \cos\left(\delta_{j,t} - \delta_{k,t}\right)\right) + \sum_{j=1}^{N} C^f P_{j,t}^{f_{DSO}} \Bigg) \end{aligned} \tag{46}$$

Where C^f objective function weight assigned by DSO on scheduled flexibility.

DSO Constraints: Distribution system nodes are subjected to the active and reactive power balance equations, as shown below:

$$\begin{aligned} P_{j,t}^{g} + P_{j,t}^{\text{Sell}_{\text{agg}}} + P_{j,t}^{f_{\text{DSO}}} - P_{j,t}^{d_{\text{agg}}} = & \sum_{k=1}^{N} V_{j,t} \cdot V_{k,t} \cdot Y_{j,k} \\ & \cos\left(\theta_{j,k} + \delta_{k,t} - \delta_{j,t}\right) \quad \forall t \in T; \forall (j,k) \in N \end{aligned} \tag{47}$$

$$\begin{aligned} Q_{j,t}^{g} + Q_{j,t}^{f_{\text{DSO}}} - Q_{j,t}^{d_{\text{agg}}} = & -\sum_{k=1}^{N} V_{j,t} \cdot V_{k,t} \cdot Y_{j,k} \\ & \sin\left(\theta_{j,k} + \delta_{k,t} - \delta_{j,t}\right) \quad \forall t \in T; \forall (j,k) \in N \end{aligned} \tag{48}$$

The right-hand sides of (47) and (48) represent the active and reactive losses on the bus j. With a constant load power factor PF of 0.85, the calculation of the reactive power and reactive flexibility requested is as follows:

$$Q_{j,t}^{d_{\text{agg}}} = \sqrt{\frac{1 - PF^2}{PF^2}} P_{j,t}^{d_{\text{agg}}} \quad \forall t \in T; \forall j \in N \tag{49}$$

$$Q_{j,t}^{f_{\text{DSO}}} = \sqrt{\frac{1 - PF^2}{PF^2}} P_{j,t}^{f_{\text{DSO}}} \quad \forall t \in T; \forall j \in N \tag{50}$$

The bus voltage and the active/reactive power obtained from the substation are also subject to the following upper and lower limits:

$$V_j^{\min} \leq V_{j,t} \leq V_j^{\max} \quad \forall t \in T; \forall j \in N \tag{51}$$

$$P_{g_j}^{\min} \leq P_{j,t}^{g} \leq P_{g_j}^{\max} \quad \forall t \in T; j = s \tag{52}$$

$$Q_{g_j}^{\min} \leq Q_{j,t}^{g} \leq Q_{g_j}^{\max} \quad \forall t \in T; j = s \tag{53}$$

The optimal flexibility request from the DSO should be less than the flexibility calculated by the aggregator. If the aggregated flexibility is positive as in (54), it implies that the users are willing to reduce their power demand. Similarly, when $P_{j,t}^{flex_{agg}}$ is negative as in (55), it indicates that users can increase the power demand. The range of flexibility request is as follows:

$$\xi^{+} \cdot P_{j,t}^{d_{agg}} \leq P_{j,t}^{f_{DSO}} \leq P_{j,t}^{flex_{agg}} \quad \forall t \in T; \forall j \in N \tag{54}$$

$$\xi^{-} \cdot \left(P_{j,t}^{sell_{agg}} + P_{j,t}^{g}\right) \leq P_{j,t}^{f_{DSO}} \leq P_{j,t}^{flex_{agg}} \forall t \in T; \forall j \in N \tag{55}$$

Where ξ^{+} and ξ^{-} are the percentage values that the DSO selects according to their requirements.

III. Optimal operation strategy of energy community based on three-stage energy management system

A. Collaborative strategies of different entities

The proposed coordination framework and strategy of the three-stage energy management system consists of the following steps, as shown in Fig. 4.

- For user: Each user has a HEMS capable of receiving settings such as customer preferences and resource parameters. The objective functions of HEMS are: 1) Minimize the total electricity cost, as shown in (1) ; 2) Minimize the total electricity consumption in the household and maximize the task laxity, as shown in (2). The HEMS schedules the distributed flexible resources twice, each targeting one of the above two objectives. Baseline demand and desired load profile can be calculated according to the two separate optimizations, and be sent to the aggregator.
- For aggregator: The aggregator accepts the optimal load demand determined by the HEMS, acting as an intermediary between multiple users and DSO, and transmitting information on decision variables. Accordingly, it has the following tasks: a) It sums up the bus-wise optimal power demand of households, and calculate the total buying and selling power between users and the DSO. b) It calculates the flexibility based on baseline demand and desired load profile of each user and aggregates the flexibility of all users on the bus. Then it also computes the flexibility index for each user, and sends the sum of upward and downward flexibility to the third stage (DSO).
- For DSO: With the aim to minimize power losses in the distribution network and the constrains of power flow, the DSO calculates the total flexibility that needs to be obtained from the aggregator at each time step. Next, the DSO sends the signal to the aggregator.
- For aggregator: The aggregator accepts the flexibility request from the DSO and performs the following tasks: a) According to the flexibility requirements sent by the DSO, it allocates the total flexibility to each user based on the flexibility index. Besides, it limits the power demand of each user within the maximum power range. b) It calculates incentive/penalty price signals based on the flexibility of each user and sends them to HEMS for rescheduling.
- For user: The end-users re-run the HEMS optimization model while using the objective function with novel incentives as shown in (3) and considering the additional constraints of maximum power limits.

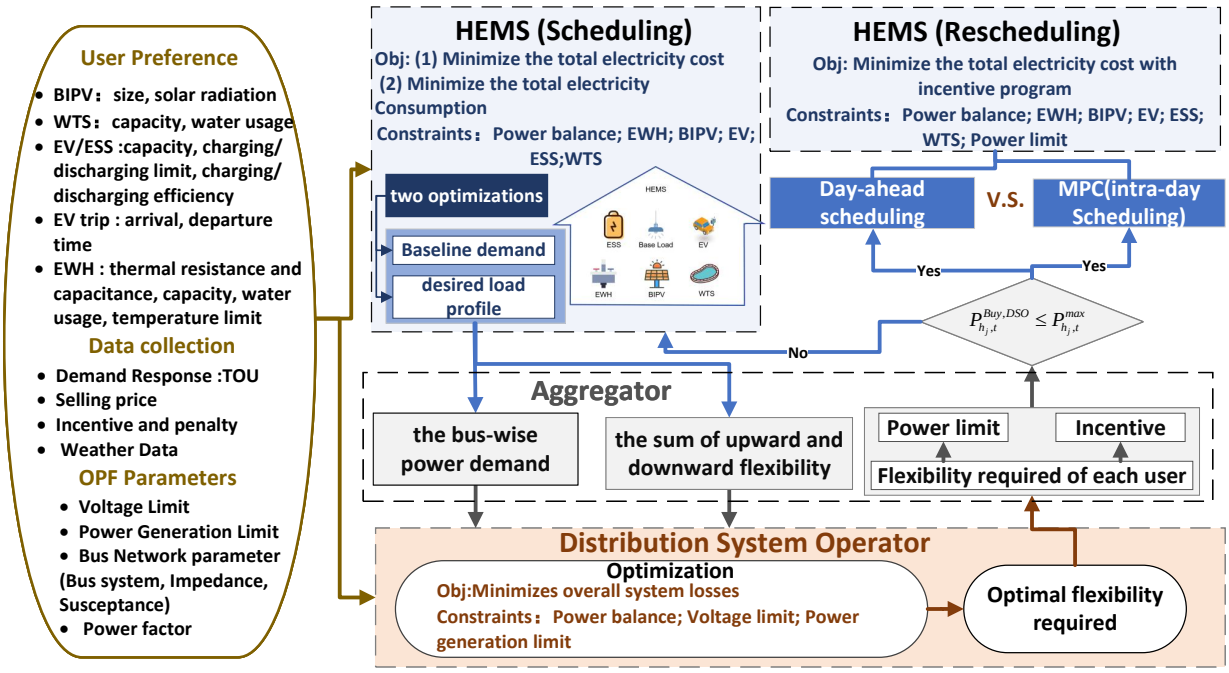

Fig. 4: Collaborative operation strategy of energy community

B. Model Predictive Control

In Model Predictive Control (MPC), an optimization problem is formulated over a finite prediction horizon. The control action is obtained by solving chosen objective function at each time-step, subject to the discrete-time model of the system and constraints. The optimal control actions minimize the objective function and thus yield the best predicted performance of the system. At the next time-step, the optimization problem is repeated with new measurements or estimates until the end of the scheduling cycle.

In this paper, the state variables for this MPC formulation include the state of charge of the reservoir, the temperatures of the EWH, the energy level of the EV and the state of charge of ESS, which is defined as $x(t) = [SoC^{\mathrm{WTS}}(t), T_l^{\mathrm{EWH}}(t), T_m^{\mathrm{EWH}}(t), T_u^{\mathrm{EWH}}(t), E^{\mathrm{EV}}(t), E^{\mathrm{ESS}}(t)]$. The control variables include the state of water pump in WTS, the power consumption of the two elements of EWH, and the charging or discharging status of ESS and EV, which is defined as $u(t) = [X^{\mathrm{WTS}}(t), P_m^{\mathrm{EWH}}(t), P_u^{\mathrm{EWH}}(t), X^{\mathrm{EV}}(t), X^{\mathrm{ESS}}(t)]$. The following optimization problem is solved at time i:

$$\min_{u(t)} \sum_{t=i}^{i+NT-1} \left(P_{h_j,t}^{\mathrm{Buy,\ DSO}}\, \pi_t^{\mathrm{Buy}} - P_{h_j,t}^{\mathrm{Sell,DSO}} \pi_t^{\mathrm{Sell}} - P_{h_j,t}^{\mathrm{Buy,DSO}} \pi_{h_j,t}^{\mathrm{Inc}} \right) \tau \tag{56}$$

subject to:

$$(4)\text{-}(33) \tag{57}$$

In this paper, the multi-time scale dispatch model for user energy management systems integrates day-ahead scheduling with rolling optimization, implementing multi-scale coordinated progressive optimization scheduling and sustainable economic operation of a three-level system. When re-runing the HEMS optimization model, the energy management system uses the results of the previous day's dispatch plan in the first stage and the optimal flexibility requirements from DSO as a reference. The system perform intra-day rolling optimisation based on MPC, gradually completing the corrections to the dispatch.

TABLE I: The Component Parameters of BIPV, WTS, and EWH

Distributed Resources	Parameters	Values
BIPV	Azimuth	0°
	tile angle	30°
	Surface reflection coefficient	0.15
	Total array power rating	5kW
	Temperature coefficient	-0.0047
WTS	Maximum water volume level	1000L
	Minimum water volume level	50L
	water pump power	2.5kW
EWH	Capacity	4.5kW
	Water tank capacity	400L
	Thermal resistance	1.52°C/kW
	Thermal capacitance	864.3kWh/°C

IV. Numerical Case Study

A. System Setup

The proposed operation strategy and optimization model of energy community is implemented on the python platform using Python Optimization Modeling Objects (PYOMO) software package. The first stage is a MILP problem that is solved using Gurobi solver. The third stage is a nonlinear programming problem, which is solved using IPOPT solver.The model is executed on a computer with Intel(R) Core(TM) Ultra9 10850H CPU@5.10 GHz processor with 32.0 GB RAM running on Windows 11 Pro 64-bit operating system. The computational time for day-ahead scheduling and MPC are 67.85s and 96.53s.

This article has been accepted for publication in IEEE Open Access Journal of Power and Energy. This is the author's version which has not been fully edited and content may change prior to final publication. Citation information: DOI 10.1109/OAJPE.2025.3549113

TABLE II: The Component Parameters of EV and ESS

	Capacity	Charging rate	Discharging rate	Charging efficiency	Discharging efficiency
EV1	19	3.3	2.8	0.89	0.91
EV2	23	6.6	4.81	0.94	0.92
ESS	46	4.5	3.8	0.86	0.85

The scheduling horizon is 24 h and begins at 9:00 AM. The selected time slot for optimization is 15 min. The component parameters of the distributed resources is given in Table I,II, as used in [16]. Some of the data employed in the case is derived from the public data sets provided by the Intelligent Systems Subcommittee of the PSACE IEEE PES [35], encompassing base load, and weather data. Other data, such as water consumption information, are obtained from simulations. The pricing scheme used in this paper is the time of use (ToU) price, and selling is a FiT price scheme, as used in [27]. The ToU pricing scheme consists of prices in three types: off-peak (0.35 yuan/kWh), mid-peak (0.6 yuan/kWh), and on-peak (1.1 yuan/kWh), and feed-in tariff is 0.495 yuan/kWh. The fixed incentives provided to the end-users is 0.72 yuan/kWh, adaptive incentives need to be calculated based on the flexibility of users at different time periods. In Figs. 6, 7, 8 and 9, the colored background is used to easily distinguish between off-peak (green shade), mid-peak (yellow shade), and on-peak (red shade) rates.

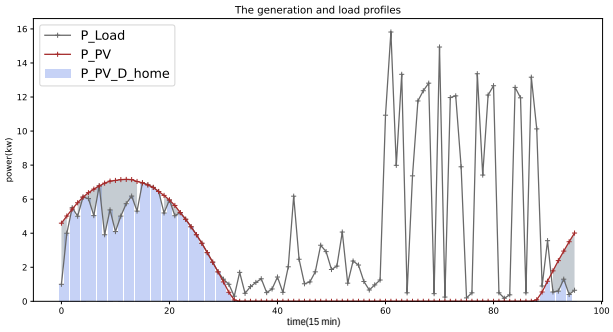

(a) Minimize cost

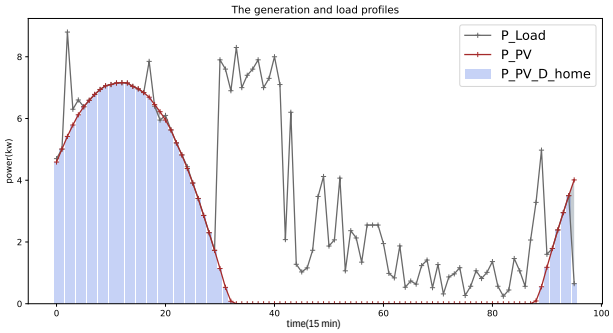

(b) Minimize Energy Consumption and maximize task laxity

Fig. 5: PV generation and load profiles

B. Method performance

1) Analysis of The Impact of Laxity: In this paper, HEMS manages a resource cluster consisting of solar PV generation, static loads, and EVs as deferrable loads. In each simulation, the load allocations are made every 15 minutes over a 24 hour operating window, so we assumes that the current renewable energy generation remains constant for the following 15-minute interval. In order to quantify the effectiveness of the scheduling policy, we focus on two quantities: renewable generation used and grid energy required. The following two objectives are used for the optimization comparison:

- Minimize cost.
- Minimize Energy Consumption and maximize task laxity.

Fig. 5 show the PV power allocation and load usage with different objective functions, which consists of the total PV generation (red curve), the user loads (grey curve), the PV generation assigned to the user loads(blue bar), and the PV generation sold to the grid for profit(grey shade). In Fig. 5(a), the PV panel generates power and can discharge power to the house, or sell to the grid, resulting in cost reductions. With the use of laxity, these plots reveal that resource scheduling can modify load profiles to closely match generation and thus reduce the need for reserves and grid energy. The laxity helps to maintain sufficient task flexibility for all active tasks, altering the real-time load distribution profile. Besides, it encourages early allocation of available generation and stops excessive delays in load demand, promoting the local consumption of new energy sources. This clearly suggests a HEMS can mitigate some of the variability associated with renewable generation through judicious allocation of power to deferrable loads.

2) Analysis of The Impact of Flexibility: DSO is responsible for managing a 33-bus distribution system. The household No.1 located at bus 9, has been selected to depict the results. In order to evaluate and showcase the performance of the proposed method, four scenarios have been considered for comparison.

- Scenario-1: HEMS without flexibility and incentive.
- Scenario-2: HEMS with flexibility and without incentive.
- Scenario-3: HEMS with flexibility and fixed incentive.
- Scenario-4: HEMS with flexibility and adaptive incentive.

When electricity prices are low, users' flexibility is mostly positive, indicating their capability and willingness to reduce power demand. During the on-peak hours, the flexibility is mostly negative, indicating that users can appropriately increase power demand to prevent rebound peaks. These upward and downward flexibilities will help the DSO upon their flexibility request to decrease or increase the power demand for a specific time Interval. The aggregated flexibility of end-users located at a bus j and the flexibility requests which DSO sends to the aggregator, as shown in Fig. 6.

Fig. 7 shows the optimal load profile of the user. When

This article has been accepted for publication in IEEE Open Access Journal of Power and Energy. This is the author's version which has not been fully edited and content may change prior to final publication. Citation information: DOI 10.1109/OAJPE.2025.3549113

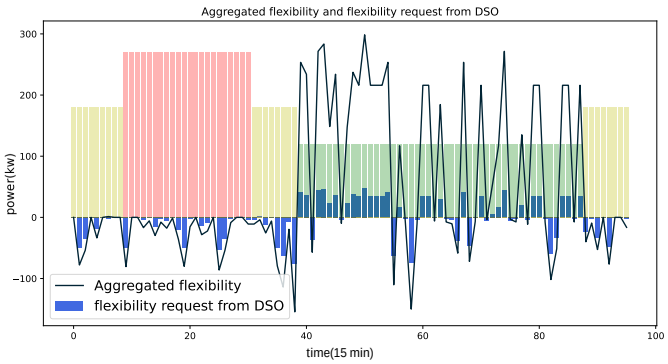

Fig. 6: Aggregated flexibility and flexibility request from DSO

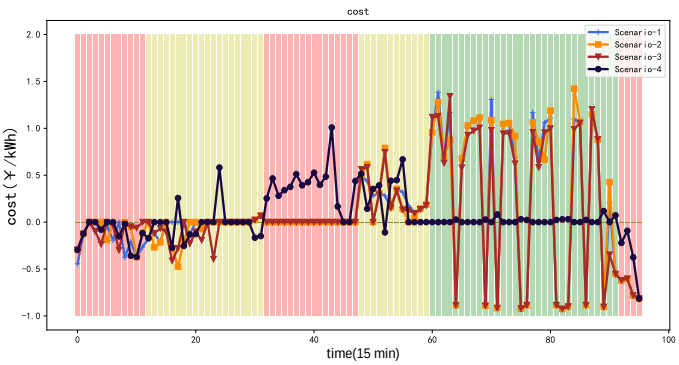

Fig. 8: Total electricity cost of houses

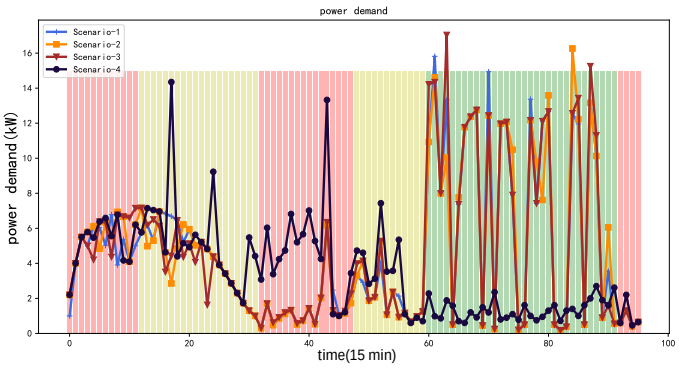

Fig. 7: Power demand of a house

the network operator provides a ToU signal, HEMS schedules controllable devices to charge at time intervals when the price is low and discharge during high-price intervals to reduce electricity costs. Consequently, rebound peaks often occur at low pricing time. The proposed method, with constraints such as maximum power limits and adaptive incentive schemes, avoids the occurrence of rebound peaks. The strategy provides timely penalties or incentives to customers, prompting them to shift their load, thus reducing peak power consumption and flattening the demand curve of the system. Reducing peak load demand and minimizing power losses can reduce the need for additional investments in grid capacity, potentially causing delay or avoiding the need for grid reinforcement. This approach also maximizes the utilization of existing network capacity.

Fig. 8 shows the electricity cost of the users per day. The result indicates that the proposed method has a minimum electricity cost compared to the other three scenarios. With flexibility and adaptive incentives, the user's cost obviously decreases, demonstrating the superiority of the strategy proposed in this paper. Compared with fixed incentives, adaptive incentives can be adjusted in real-time based on user flexibility at different times for better load regulation, thus maximizing benefits. The proposed method reduces the electricity cost of the overall system by 26.26%, relative to the base case. Similarly, the peak load has been reduced by 9.28%, as in Table III.

C. Comparison with Model Predictive Control

The prediction horizon of the MPC problem is 24 hours and the sampling time is 5 minutes. In this paper, we compare the scheduling results of day-ahead scheduling plans and intra-day rolling optimization to test the performance of MPC and the effectiveness of the flexibility index.

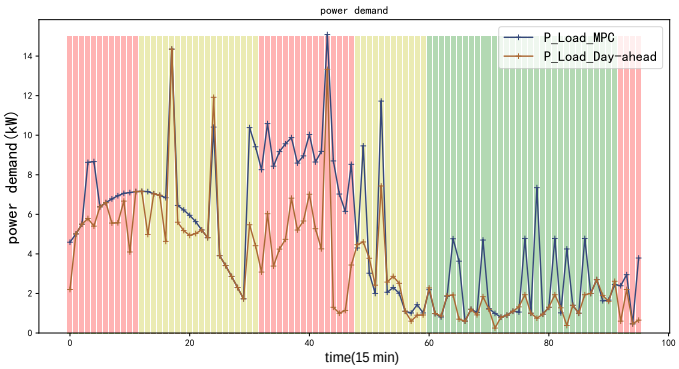

Fig. 9: Power demand of a house for Day-ahead scheduling and MPC

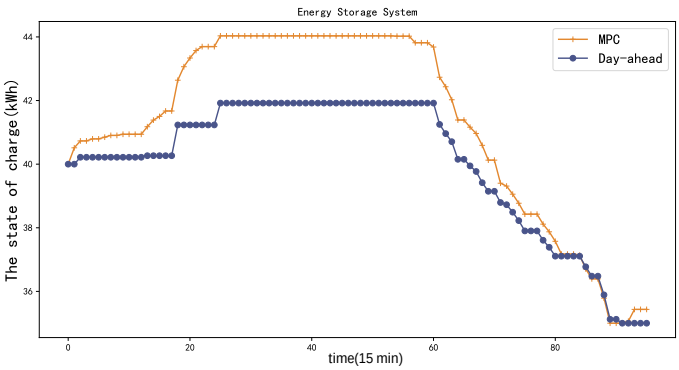

Fig. 10: The state of charge of ESS for Day-ahead scheduling and MPC

Based on the day-ahead output plan, the user forms operation strategies based on predictions of real-time electricity prices and load variation. Therefore, the load profile of intra-day scheduling using MPC, as shown in Fig. 9, follows the

trend of the day-ahead schedule, and some minor adjustments are made to improve the accuracy of the dispatch by considering the uncertainties of renewable energy sources or customer activities. It results in a decrease in user costs and peak loads compared to day-ahead scheduling, and achieves an increase in user revenues.

ESS has significant load shifting capabilities due to its large capacity, therefore the MPC rationally allocates the charging or discharging time of ESS to fully utilise the energy capacity. The comparison of the state of charge of ESS for different control strategies is depicted in Fig. 10. Results are included in Table III for the total electricity cost and peak load information, showing how the cost and the peak load varies as a function of flexibility indicators and MPC method. compared to the base case. Compared with the day-ahead schedule, the MPC method performs a more economical operation and obtains a higher profit, resulting in 35.14% cost reduction relative to the Scenario-1. Most of these cost reductions are driven by a shift in load from on-peak to off-peak pricing periods, as opposed to improvements in energy efficiency. Moreover, the peak load of the overall system has been reduced by 16.61%, compared to scenario-1. Peak reduction prevents system components from reaching thermal overload, facilitating congestion management and postponing the need for grid reinforcement.

TABLE III: The Total Electricity Cost and Peak Load Information

	Day-ahead scheduling				MPC
Scenario	1	2	3	4	\
The cost for electricity purchase(yuan)	23.8963	23.6181	29.5968	24.5528	23.2154
The profit for selling electricity(yuan)	15.2157	14.9875	22.5149	18.1520	17.5848
The net cost(yuan)	8.6807	8.6306	7.0819	6.4008	5.6306
The value of peak load(kW)	15.8176	14.457	17.035	14.35	13.19

V. Conclusion

In this paper, the optimal operation strategy of an energy community aggregator for heterogeneous distributed flexible resources is proposed to offer a unique and comprehensive solution to the challenges of DER integration in the grid. A three-level framework among DSOs, aggregators, and HEMS, is developed specially using flexibility indicators including the flexibility of load variation and the task laxity to assess the techno-economic performance of the energy management system. The adaptive incentive based on flexibility encourages the users to shift load demands to non-peak hours, and resource scheduling with the laxity factor results in aggregate load profiles that better accommodate the renewable generation profile. The multiple-time-scale dispatch strategy that employs MPC algorithm updates the state of flexible resources in real time and minimizes the influence of the prediction error. The simulation results show that the proposed method can help reshape the load profiles and reduce the overall maintenance cost and the maximum load by 35. 14% and 16. 61%, respectively, demonstrating the statistically almost guaranteed long-term economic benefit.

Future work could focus on developing the architecture by adding dynamic models of other controllable distributed resources and considering the long-term impacts of factors like battery degradation or infrastructure installation and maintenance costs. Furthermore, more studies can evaluate the model with other flexibility indices and modeled the user-side energy management system in larger energy communities under various scenarios, such as different extreme weathers and seasons. The scalability of the optimal operation strategy based on the flexibility to larger energy communities and the sensitivity analysis to explore how key parameters influence the outcomes is also within the scope of future work.

References

[1] D. Watari, I. Taniguchi, and T. Onoye, "Duck curve aware dynamic pricing and battery scheduling strategy using reinforcement learning," *IEEE Transactions on Smart Grid*, vol. 15, no. 1, pp. 457–471, 2024.

[2] E. Rodriguez-Diaz, E. J. Palacios-Garcia, M. Savaghebi, J. C. Vasquez, and J. M. Guerrero, "Development and integration of a hems with an advanced smart metering infrastructure," in *2016 IEEE International Conference on Consumer Electronics (ICCE)*, 2016, pp. 544–545.

[3] F. Luo, W. Kong, G. Ranzi, and Z. Y. Dong, "Optimal home energy management system with demand charge tariff and appliance operational dependencies," *IEEE Transactions on Smart Grid*, vol. 11, no. 1, pp. 4–14, 2020.

[4] S. Xu, X. Chen, J. Xie, S. Rahman, J. Wang, H. Hui, and T. Chen, "Agent-based modeling and simulation for the electricity market with residential demand response," *CSEE Journal of Power and Energy Systems*, vol. 7, no. 2, pp. 368–380, 2020.

[5] T. Xu, T. Chen, C. Gao, and H. Hui, "Intelligent home energy management strategy with internal pricing mechanism based on multiagent artificial intelligence-of-things," *IEEE Systems Journal*, 2023.

[6] T. Chen, Q. Alsafasfeh, H. Pourbabak, and W. Su, "The next-generation us retail electricity market with customers and prosumers—a bibliographical survey," *Energies*, vol. 11, no. 1, p. 8, 2018.

[7] T. Xu, T. Chen, C. Gao, and H. Hui, "Intelligent home energy management strategy with internal pricing mechanism based on multiagent artificial intelligence-of-things," *IEEE Systems Journal*, vol. 17, no. 4, pp. 6045–6056, 2023.

[8] F. Sangoleye, J. Jao, K. Faris, E. E. Tsiropoulou, and S. Papavassiliou, "Reinforcement learning-based demand response management in smart grid systems with prosumers," *IEEE Systems Journal*, vol. 17, no. 2, pp. 1797–1807, 2023.

[9] J. A. Marcelo, G. Muñoz-Delgado, D. Rupolo, J. Contreras, and J. R. Mantovani, "Multistage planning for active power distribution systems with increasing penetration of prosumers and electric vehicles," *Sustainable Energy, Grids and Networks*, vol. 38, p. 101280, 2024.

[10] J. Hu, J. Wu, X. Ai, and N. Liu, "Coordinated energy management of prosumers in a distribution system considering network congestion," *IEEE Transactions on Smart Grid*, vol. 12, no. 1, pp. 468–478, 2021.

[11] Y. Fu, W. Xu, Z. Wang, S. Zhang, X. Chen, and X. Zhang, "Experimental study on thermoelectric effect pattern analysis and novel thermoelectric coupling model of bipv facade system," *Renewable Energy*, vol. 217, p. 119055, 2023.

[12] G. Xinxin, S. Qi, Z. Mingfeng, Z. Qi, L. Shuangshou, and L. Weiran, "Operation optimization strategy of a bipv-battery storage hybrid system," *Results in Engineering*, vol. 18, p. 101066, 2023.

[13] I. Boukas, E. Burtin, A. Sutera, Q. Gemine, B. Pevee, and D. Ernst, "Exploiting the flexibility potential of water distribution networks: A pilot project in belgium," *IEEE Transactions on Smart Grid*, vol. 15, no. 1, pp. 394–404, 2024.

[14] T. Peirelinck, C. Hermans, F. Spiessens, and G. Deconinck, "Domain randomization for demand response of an electric water heater," *IEEE Transactions on Smart Grid*, vol. 12, no. 2, pp. 1370–1379, 2021.

[15] E. Buechler, A. Goldin, and R. Rajagopal, "Improving the load flexibility of stratified electric water heaters: Design and experimental validation of mpc strategies," *IEEE Transactions on Smart Grid*, vol. 15, no. 4, pp. 3613–3623, 2024.

[16] U. Kumar Jha, N. Soren, and A. Sharma, "An efficient hems for demand response considering tou pricing scheme and incentives," in *2018 2nd International Conference on Power, Energy and Environment: Towards Smart Technology (ICEPE)*, 2018, pp. 1–6.

[17] P. Faria, J. Spínola, and Z. Vale, "Aggregation and remuneration of electricity consumers and producers for the definition of demand-response programs," *IEEE Transactions on Industrial Informatics*, vol. 12, no. 3, pp. 952–961, 2016.

[18] M. A. Fotouhi Ghazvini, J. Soares, O. Abrishambaf, R. Castro, and Z. Vale, "Demand response implementation in smart households," *Energy and Buildings*, vol. 143, pp. 129–148, 2017.

[19] O. Alrumayh and K. Bhattacharya, "Flexibility of residential loads for demand response provisions in smart grid," *IEEE Transactions on Smart Grid*, vol. 10, no. 6, pp. 6284–6297, 2019.

[20] F. Lezama, J. Soares, B. Canizes, and Z. Vale, "Flexibility management model of home appliances to support dso requests in smart grids," *Sustainable Cities and Society*, vol. 55, p. 102048, 2020.

[21] D. Aussel, L. Brotcorne, S. Lepaul, and L. von Niederhäusern, "A trilevel model for best response in energy demand-side management," *European Journal of Operational Research*, vol. 281, no. 2, pp. 299–315, 2020.

[22] L. Li, "Coordination between smart distribution networks and multi-microgrids considering demand side management: A trilevel framework," *Omega*, vol. 102, p. 102326, 2021.

[23] Z. Lu, H. Li, and Y. Qiao, "Probabilistic flexibility evaluation for power system planning considering its association with renewable power curtailment," *IEEE Transactions on Power Systems*, vol. 33, no. 3, pp. 3285–3295, 2018.

[24] M. Z. Degefa, I. B. Sperstad, and H. Sæle, "Comprehensive classifications and characterizations of power system flexibility resources," *Electric Power Systems Research*, vol. 194, p. 107022, 2021.

[25] A. Subramanian, M. J. Garcia, D. S. Callaway, K. Poolla, and P. Varaiya, "Real-time scheduling of distributed resources," *IEEE Transactions on Smart Grid*, vol. 4, no. 4, pp. 2122–2130, 2013.

[26] H. Wang, C. Zhang, K. Li, S. Liu, S. Li, and Y. Wang, "Distributed coordinative transaction of a community integrated energy system based on a tri-level game model," *Applied Energy*, vol. 295, p. 116972, 2021.

[27] S. Hussain, O. Alrumayh, R. P. Menon, C. Lai, and U. Eicker, "Novel incentive-based multi-level framework for flexibility provision in smart grids," *IEEE Transactions on Smart Grid*, vol. 15, no. 2, pp. 1594–1607, 2024.

[28] T. Xu, T. Chen, C. Gao, M. Song, Y. Wang, and H. Yuan, "Distributed flexible resource regulation strategy for residential communities based on deep reinforcement learning," *IET Generation, Transmission & Distribution*, vol. 18, no. 21, pp. 3378–3391, 2024.

[29] J. Vasilj, S. Gros, D. Jakus, and M. Zanon, "Day-ahead scheduling and real-time economic mpc of chp unit in microgrid with smart buildings," *IEEE Transactions on Smart Grid*, vol. 10, no. 2, pp. 1992–2001, 2019.

[30] Z. Li, L. Wu, Y. Xu, S. Moazeni, and Z. Tang, "Multi-stage real-time operation of a multi-energy microgrid with electrical and thermal energy storage assets: A data-driven mpc-adp approach," *IEEE Transactions on Smart Grid*, vol. 13, no. 1, pp. 213–226, 2022.

[31] A. Parisio, C. Wiezorek, T. Kyntäjä, J. Elo, K. Strunz, and K. H. Johansson, "Cooperative mpc-based energy management for networked microgrids," *IEEE Transactions on Smart Grid*, vol. 8, no. 6, pp. 3066–3074, 2017.

[32] C. Chen, J. Wang, Y. Heo, and S. Kishore, "Mpc-based appliance scheduling for residential building energy management controller," *IEEE Transactions on Smart Grid*, vol. 4, no. 3, pp. 1401–1410, 2013.

[33] T. Mutaz, A. A. Jadallah, G. A. Bilal, and O. M. Abdulmajeed, "Virtual performance evaluation of net-zero energy building (nzeb) using bim analysis," in *2022 Muthanna International Conference on Engineering Science and Technology (MICEST)*, 2022, pp. 169–173.

[34] Q. Peng, W. Li, M. Fowler, T. Chen, W. Jiang, and K. Liu, "Battery calendar degradation trajectory prediction: Data-driven implementation and knowledge inspiration," *Energy*, p. 130849, 2024.

[35] "Open data sets - ieee pes intelligent systems subcommittee," https://site.ieee.org/pes-iss/data-sets.